Aerodynamical phenomena in a large top covered wind mill with vertical axis wind turbine

Abderrahmane Baïri
Université de Paris, Laboratoire Thermique Interfaces Environnement (LTIE EA 4415), Ville d'Avray, France
Cyril Crua
School of Computing, Engineering and Mathematics, University of Brighton, Brighton, UK
Jean-Gabriel Bauzin
Laboratoire Thermique Interfaces Environnement (LTIE EA 4415), Ville d'Avray, France, and
Iken Baïri
Université de Paris, Laboratoire Thermique Interfaces Environnement (LTIE EA 4415), Ville d'Avray, France

Received 25 November 2014
Revised 14 January 2015
Accepted 15 January 2015

Abstract

Purpose – The purpose of this paper is to examine the aerodynamical and air mass flow phenomena taking place in the channel of a modified version of one of the well-known Sistan wind mills, in order to improve its aerodynamic performance.

Design/methodology/approach – The simulations are done by means of the finite volume method associated to the realizable k-ε turbulence model. The computational domain consists in a rotating sub domain including the wind turbine equipped with nine blades and a fixed sub domain including the rest of the computational domain. Both are connected by means of a sliding mesh interface. Calculations are done for 8×10^5-4×10^6 Reynolds number range, corresponding to inlet velocities varying from 2 to 10 m s^{-1}.

Findings – The velocity fields are presented for the stopped and operating turbine (static and dynamic conditions). A careful examination of the aerodynamic phenomena is performed to detect potential vortices that could develop in the central cavity of the active assembly, and then influence the wind turbine's operation.

Originality/value – The modification proposed in this survey is easy to realize, consisting in covering the top of the entire original assembly that avoids the extraction of a large part of the air mass flow occurring through the open top of the original version. The aerodynamic phenomena occurring across the channel of this large vertical axis wind turbine are substantially different from those of the original version.

Keywords Finite volume method, Aerodynamics, Applied fluid dynamics, Vertical axis wind turbine (VAWT), Wind mill, Air mass flow

Paper type Research paper

Nomenclature

D	diameter of the wind turbine (m)	$Q_{x,\,d}$	local air mass flow in dynamic mode (kg s^{-1})
H	cavity's height (m)	Re	Reynolds number (–)

International Journal of Numerical Methods for Heat & Fluid Flow
Vol. 26 No. 1, 2016
pp. 365-378

0961-5539
DOI 10.1108/HFF-11-2014-0350

U_{in}	inlet velocity ($m\,s^{-1}$)	δ	deviation $\delta = 100$ $(U_{max,\,d} - U_{max,\,s})/U_{max,\,d}$ (%)
U_d, U_s	air velocity in dynamic and static modes respectively ($m\,s^{-1}$)	μ	air dynamic viscosity (Pa s)
$U_{max,\,d}$, $U_{max,\,s}$	maximum air velocity for the dynamic and static modes respectively ($m\,s^{-1}$)	ν	air kinematic viscosity ($m^2\,s^{-1}$)
x, y, z	Cartesian coordinates (m)	ρ	air density ($kg\,m^{-3}$)
z^*	dimensionless coordinate $z^* = z/H(-)$	ω_{wt}, ω_{nt}	angular velocity for configurations with and without top cover ($rd\,s^{-1}$)
Greek symbols			
α	angle with respect to the direction "Ox"		

1. Introduction

This study considers the aerodynamical phenomena that occur in a modified version of one of the well-known Sistan-type wind mills in order to improve its aerodynamic performance. The modification proposed in the present survey is easy to realize. The top of the entire assembly is covered whereas it is open in the original version, constituting an outlet for a large part of the air mass flow, and thus reducing the torque of the wind turbine's rotor. Several works deal with wind mills. The technological and architectural features as well as the economical and development perspective aspects related to wind energy are presented in various works such as those of Joselin Herberta *et al.* (2007) and Rapin and Noël (2010, 2014). Some details concerning the Vertical Axis Wind Turbine (VAWT) considered in the present survey are treated by Bhutta *et al.* (2012) and Islam *et al.* (2008). The numerical solutions by means of CFD have been greatly improved in recent years thanks to the increasingly suitable computing methods and specific algorithms. The problems in wind energy involve significant computing resources because the elaborated and large considered geometries require implementing complex and moving meshes, and a high number of elements. Correct simulation of the aerodynamic and thermal phenomena is done by means of specific turbulence models and calculation procedures. These aspects are discussed by Islam *et al.* (2008) who also present experimental techniques to determine the VAWT characteristics and performance. The Sistan wind mill type is considered as one of the oldest. Many works, including those of Joselin Herberta *et al.* (2007), Shepherd (1990), Al-Hassan and Hill (1986), Hau (2006), Campbell (2011) have focussed on its technical, architectural and economic specifications. The aerodynamical aspects are treated by Muller *et al.* (2009) who proposed solutions to improve the performance of the traditional version by adding disks at top and bottom of the rotor, and by increasing the number of turbine blades. The study concludes that more research should be done to optimize its performance. This machine could be integrated in some modern buildings' design to reduce fossil fuel consumption and CO_2 emissions in order to preserve the environment. The concept of a small VAWT is examined in many works such as Sharpe and Proven (2010) for its integration in the building conception. The numerical approach by Arfaie *et al.* (2014) examines the effect of the roughness on the turbulent flow in a 2D channel. The Reynolds Averaged Navier-Stokes (RANS) equations are solved for Reynolds numbers varying from 6.3×10^3 to 4.5×10^4, by using the Ansys-Fluent code (Ansys CFX v14 Help

Manuals, 2011). The survey shows the influence of the roughness spacing to height ratio on the flow and the heat transfer phenomena. This aspect has been studied in other works such as that of Liou *et al.* (1993) and the experimental part of the survey by Okamoto *et al.* (1993) who demonstrated the direct relationship between heat transfer and turbulence intensity. The wind turbulence effect on wind-driven rain is examined numerically by Abadie and Mendes (2008) by means of an Eulerian Second Moment Closure and a Lagrangian one-way coupling models. The 3D model applied to building domain shows that turbulence can be neglected for some dynamic configurations. The aerodynamic phenomena related to the interference between the tower and the blades in the case of a horizontal axis upwind wind turbine has been investigated by Lin and Shieh (2010). Their numerical survey is based on the shear stress transport (SST) k-ω turbulence model. The meshing of the computational domain is composed of a fixed part (tower) and a mobile one (sliding blade). The 3D transient numerical approach used by Kadja *et al.* (1996) based on partially covered boundary cells confirms the influence of the topography on the wind flow characteristics. This study based on the finite-volume method can predict the dispersion of pollutants in urban and industrial areas and in roads depending on the complexity of the field. The numerical study of Cohen and Ryan (1985) uses a formulation dealing with the non-breaking wave regime and restricted to conditions of a fully turbulent water drift current. The calculated results are in good agreement with some experimental data and previous empirical correlations. The meshing plays an essential role for the numerical simulation of aerodynamic and thermal phenomena that occur in the channel of the wind turbine. This is important since the computational domain is typically very extended, which requires a large number of elements. The mesh is also often irregular to take into account the different areas in which the phenomena are very different, in relation with the local velocity characteristics. Several studies have been devoted to optimizing the mesh on the computational domain in order to minimize the computation time while preserving results quality. The mesh optimization is particularly important in the majority of works where various methods are implemented according to the considered problem. The General Richardson Extrapolation method appears to be adapted to the VAWT investigated by Almohammadi *et al.* (2013) and the fitting method is interesting because it does not require a too dense mesh. However, the Grid Convergence Index method is not recommended. The turbulence, omnipresent in most applications in wind energy is systematically taken into account. Several models are available, more or less adapted to the considered problem. The work of Baïri *et al.* (2015) contains some details of the main models used in thermal and aerodynamics fields, with their advantages and disadvantages. The unsteady 2D numerical approach by Almohammadi *et al.* (2013) uses the ReNormalized Groups (RNG) k-ε as well as the SST turbulence models. The standard k-ε turbulence model associated to logarithmic surface function is used in the study by Altan and Atılgan (2008) where a Savonius wind rotor is considered. To reduce the torque that occurs on the convex blade of the rotor in the negative direction, a deflector is installed in front of the rotor. The realizable k-ε turbulence model associated to the SIMPLC algorithm has been used by Cao *et al.* (2012) to calculate the 2D unsteady incompressible flow for a VAWT. The authors describe the effects of the wind turbine's rotational velocity on the turbulent kinetic energy. The experimental study by Kim and Gharib (2013) shows that the relative position of an upstream deflector has a clear influence on the power output of two counter-rotating straight-bladed VAWTs, and a single turbine. The 2D and 3D models developed by McTavish *et al.* (2012) are associated to the k-ε and RNG turbulence models.

The aerodynamic characteristics are determined in the study of Howell *et al.* (2010) by a 2D and 3D unsteady numerical models. The comparison between the results of both calculations were compared to measurements. Only the 3D model is able to correctly simulate the resulting flows. The experimental survey of Irabu and Roy (2007) done with a guide-box tunnel consists in determining some characteristics as the static (fixed rotor) and dynamic (rotating rotor) torques as well as the output power of a Savonius rotor under various dynamic conditions. The optimum value of spacing ratio between the rotor tip and the side walls has been determined, and a comparison between results of the maximum output power coefficient concerning two and three blades rotor is presented. Some details of the aerodynamic phenomena occurring in an initial version of the Sistan-type wind mill are treated in the numerical survey by Baïri (2014) for Reynolds numbers ranging from 8×10^5 to 4×10^6. The finite volume method is used, while the turbulence is treated with the realizable k-ε model.

The present study examines a modified version of this wind mill, by covering the top of the whole assembly, given that the top in the original version is open. This simple and easy to realize modification improves the wind mill aerodynamic performance. Calculations are done by means of the finite volume method associated to the realizable k-ε turbulence model. The same Reynolds number range treated by Baïri (2014) is considered, corresponding to inlet velocities varying from 2 to 10 m s^{-1}. The computational domain consists of a rotating sub domain including the wind turbine equipped with nine blades and a fixed sub domain including the rest of the computational domain. Both are connected by means of a sliding mesh interface. The velocity fields are presented for the stopped and operating turbine (static and dynamic conditions). A careful examination of the aerodynamic phenomena is performed to detect potential vortices that could be present in the central cavity of the active assembly, and thus influence the wind turbine's operation. Finally, for easier comparison of this work's results with those of Baïri (2014) concerning the same assembly without the cover, the present survey is presented with the same structure.

2. The considered assembly. Numerical procedure

The wind mill (5 m height, 7 m depth, 18 m width) considered in this survey is presented in Figure 1(a). The air collected at the inlet section: with U_{in} velocity is oriented by the deflector; and introduced into the central cavity containing the wind turbine's rotor; the whole assembly is covered by a rigid plate Figure 1(b). This is not the case in the original version discussed by Baïri *et al.* (2016) for which the top is

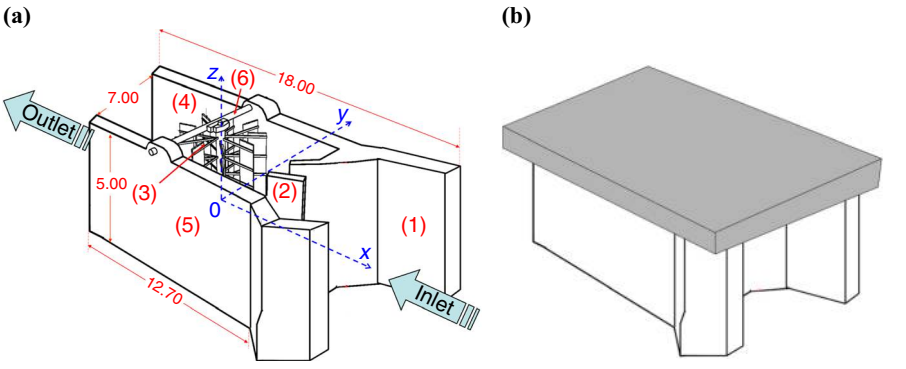

Figure 1.
The considered assembly details

Notes: (a) Topless; (b) with top

not covered. With this configuration, the air leaves the cavity exclusively by the rear "*yz*" section, whereas in the original version, a large part of the air flow leaves through the top. The channel is delimited by the floor and two vertical walls denoted; and; the rotor's axis is maintained at its upper part by a crossbar; the origin of the Cartesian reference used in this study is centered in the middle of the turbine axis as shown in Figure 1(a). The considered domain whose top view is presented in Figure 2 is asymmetrical and oriented in the prevailing local wind's direction.

The rotor is equipped with nine plane blades of 3 m length numbered from 1 to 9 as indicated in Figure 2 which contains also the dimensions and some details of the assembly. Each blade is covered at its extremity over only 1 m width (Figure 3(e)), and the remaining part is open. The 647,438 elements constituting the domain's walls are unstructured to facilitate the mesh adaptation to the treated geometry. As presented in Figure 3, the number of elements is irregularly distributed on the walls to reflect the more or less complex local dynamic phenomena. The top wall shown in Figure 3(c) is not meshed with the function adopted for the upper fluid boundary concerning the original version considered by Baïri *et al.* (2016) because the aerodynamic phenomena are substantially different in the two versions. The fluid computational domain is unstructured, constituted by 318,921 tetrahedral cells and 59,133 nodes.

The distribution is uniform in the inlet and outlet sections. The mesh at interfaces between the blades and the floor, and between the blades and the top cover has been tightened by means of the near-wall concentration function. This optimized mesh is the result of various tests ensuring a reasonable computing time associated to a satisfactory precision. This mesh is denser than the one adopted for the open cavity by Baïri (2014), optimized with 622,239 elements, 305,188 cells and 56,750 nodes. This 4 percent increase is mainly due to the larger average air flow impulsion (see the velocity field below) for the case discussed in this work, thanks to the top cover. This optimized mesh is based on impulsion balances done at seven representative "*yz*" sections numbered from 1 to 7 in Figure 4, whose corresponding abscissa are $x = -6.2$, -4.0, 0.0, $+4.0$, $+6.2$, $+7.1$ and

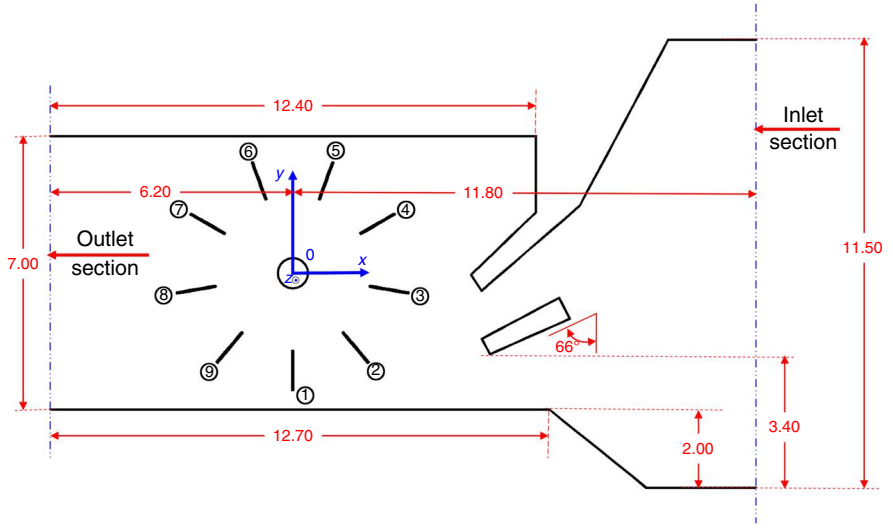

Note: Dimensions are given in meters

Figure 2.
The considered domain

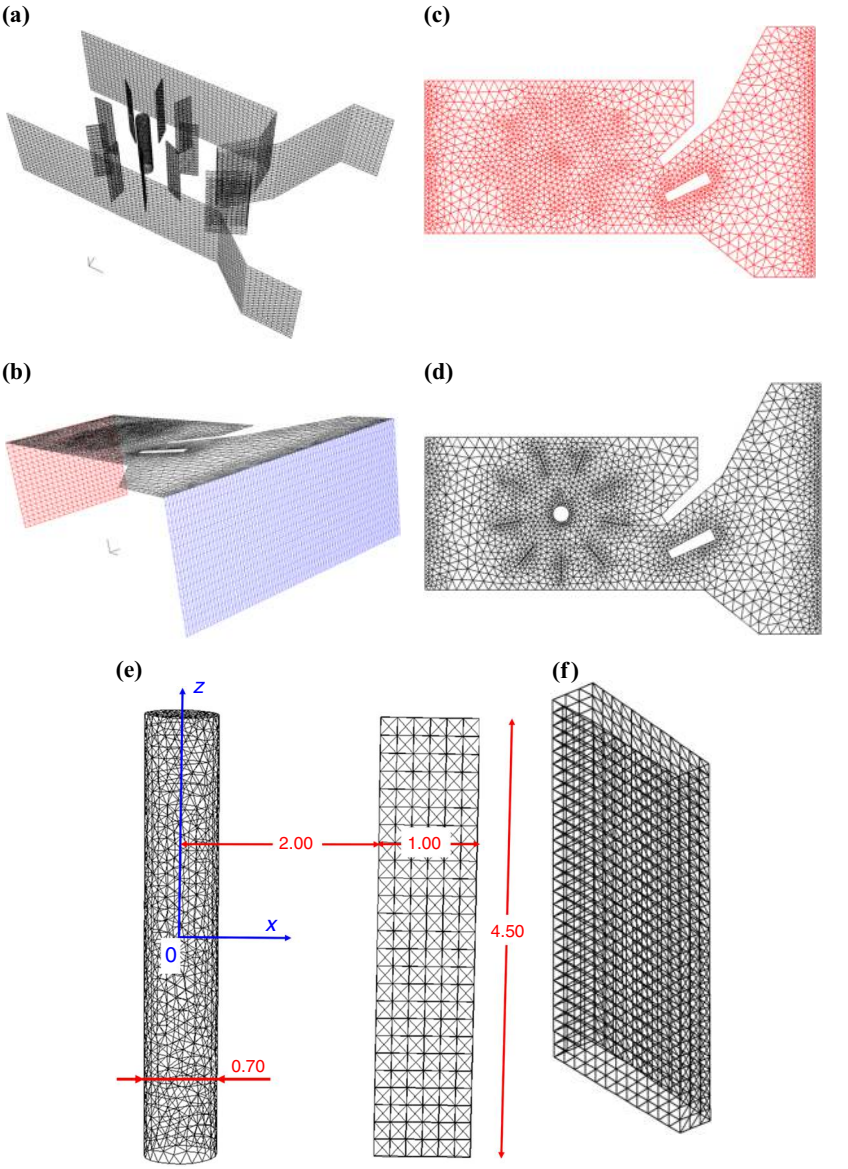

Figure 3.
The adopted mesh

Notes: (a) Collector, deflector, rotor with blades, right and left vertical walls; (b) inlet section (blue color), outlet section (red color) and top cover (black color); (c) top cover details; (d) floor details; (e) the rotor's axis and one blade; (f) the deflector

+11.8 m, respectively. The convergence criterion is set to 10^{-5}. The adopted mesh independence has been checked with the techniques used in this field, detailed by Almohammadi *et al.* (2013). The angle α referenced with the "Ox" direction in Figure 4 allows identifying some areas in which particular aerodynamical phenomena may occur.

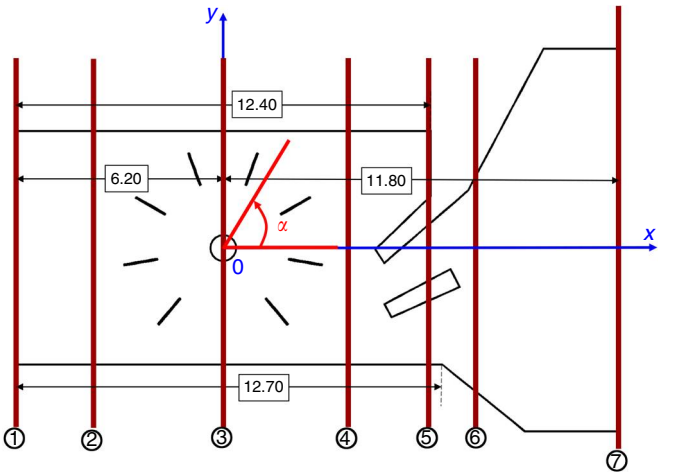

Notes: Distances in meters. $x = -6.2$, -4.0, 0.0, +4.0, +6.2, +7.1 and +11.8 m for section 1-7, respectively

Figure 4.
The "*yz*" sections to determine the air mass flow and impulsion balances

The computational domain used for the airflow simulation during the operation of the wind turbine is composed of two sub domains. The rotating one includes the wind turbine and the fixed sub domain considers the rest of the computational domain. Both are connected by means of the Sliding Mesh interface technique.

All calculations are performed in transient regime, but only results at steady state are taken into account. In the initial state, the pressure is equal to 10^5 Pa (standard atmospheric pressure), the whole assembly is isothermal at 20°C and the air is quiescent. The dynamic viscosity and density of the airflow are kept constant ($\mu = 1.8205 \times 10^{-5}$ Pa s; $\rho = 1.2047$ kg m^{-3}) during the calculation process. Reynolds numbers $Re = U_{in}D/v$ (based on the diameter as the characteristic length) vary from 8×10^5 to 4×10^6, corresponding to the five air inlet velocity U_{in} values considered in this survey (2, 4, 6, 8 and 10 m s^{-1}).

Weight and "O*z*" component of the mass moment of inertia of the wind turbine's rotor are set to 1,000 kg and 10,000 kg m^2, respectively. The pressure condition is adopted at the outlet section, while the non-slip condition is imposed on all internal walls, including the blades. Simulations are done in 3D because a 2D approach cannot correctly simulate the airflows given the asymmetric, large and complex treated geometry.

The classic 3D RANS governing equations are solved by means of the Ansys-Fluent software (Ansys CFX v14 Help Manuals, 2011) based on the finite volume method. This system is widely described in several works including those of Anderson (1995) and Versteeg and Malalasekara (1995). The SIMPLE algorithm is adopted for the pressure-velocity coupling in the momentum equations. The time step is 50 ms, the convergence criteria is set to 10^{-5} and turbulence is treated by means of the realizable k-ε model which has been implemented in most similar works, given its easy implementation, good performance and reasonable computing time. This model is recommended for calculations including rotating fields as it is the case in the present work. Some details of the different turbulence models used in the aerodynamic field are presented in various works as those of Muller *et al.* (2009) and Baïri *et al.* (2015).

3. Main results

As in the study by Baïri (2014), the calculations show that the flow velocity in the channel have the same trend for the five considered inlet velocities $U_{in} = 2, 4, 6, 8$ and $10\,m\,s^{-1}$. This observation concerns the dynamic and the static cases. These fields are presented in Figure 5 in the center of the turbine's axis ($z^* = 0$), for both static and dynamic wind turbine (U_s and U_d, respectively). The maximum velocity is specified for each case. The values are systematically larger for the static case, unlike the case of the open cavity (maximum for dynamic case). The difference is however very low and not significant. As shown in Figure 6, the deviation $\delta = 100(U_{max,d} - U_{max,s})/U_{max,d}$ between $U_{max,d}$ and $U_{max,s}$ corresponding to the maximum velocity values for the

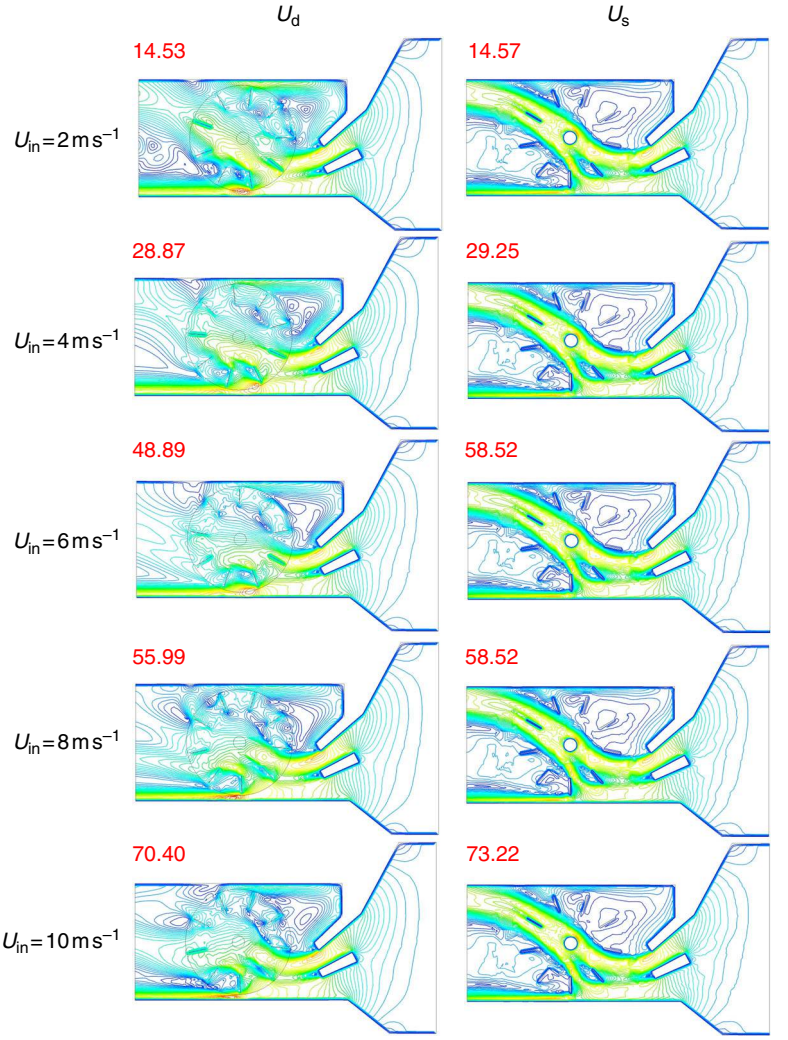

Figure 5.
Velocity fields at $z^* = 0$ for $U_{in} = 2$, 4, 6, 8 and $10\,m\,s^{-1}$

Notes: The maximal values are indicated for all the cases ($m\,s^{-1}$). Dynamic (U_d) and static (U_s) wind turbine

dynamic and static turbine equals 0.41, 1.33, 0.04, 4.32 and 3.85 percent for $U_{in} = 2$, 4, 6, 8 and 10 m s^{-1}, respectively.

This difference is higher for the original version of the wind mill (without top cover). It is about 25 percent for 2 m s^{-1} and decreasing with increasing U_{in}, reaching 5.3 percent for 10 m s^{-1}. The airflow is substantially influenced by the rotation of the wind turbine. Two main flow directions are observed in the dynamic configuration. The first one is located on the left wall, as a consequence of the deflector orientation. The second concerns the volume enclosing the turbine itself. Throughout the rest of the central cavity, the flow is very low for all the considered U_{in} values.

The rotor's angular velocity ω_{wt} concerning the dynamic wind turbine has been calculated by taking into account the weight and the "Oz" component of the mass moment of inertia previously specified. Its value is compared to those corresponding to the original version treated by Baïri (2014) denoted ω_{nt}.

The results presented in Figure 7 show that angular velocities are considerably higher for the version with a top. The ratio of the angular velocities with and without top is of about 3.5. The linear functions $\omega_{wt} = 2.2324 U_{in}$ and $\omega_{nt} = 2.6337 U_{in}$ represent the evolution of ω_{wt} and ω_{nt} vs U_{in} with determination coefficients greater than 0.998.

Examination of the flow in the central cavity confirms that the vortices are not more numerous than for the open-top cavity. The example presented in Figure 8(a) for $U_{in} = 10$ m s^{-1} shows that the stationary vortices located on both sides of the interface between the fixed and mobile sub domains are very low and their clockwise rotation

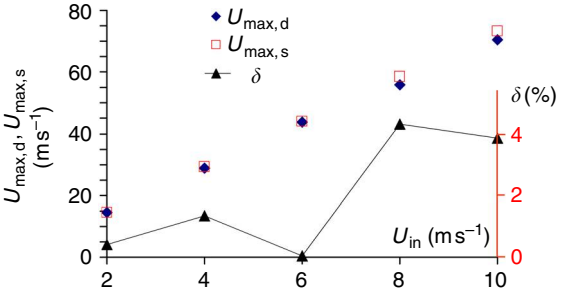

Note: Deviation δ for $2 \leqslant U_{in} \leqslant 10$ m s^{-1}

Figure 6.
Evolution of maximum velocity airflow $U_{max,\,d}$ and $U_{max,\,s}$ vs U_{in} for the dynamic and static turbine, respectively

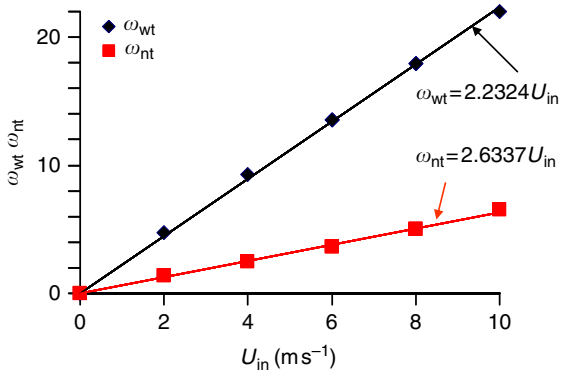

Figure 7.
Evolution of ω_{wt} and ω_{nt} vs U_{in}

does not cause interference with the rotor's operation. The same observation concerns the vortex located outside the volume enclosing the turbine for $U_{in} = 2\,m\,s^{-1}$ presented in Figure 8(b).

For all the cases treated in this work, the forces generated by the flow on the blades produce a positive rotor moment (Figure 8(c) for $U_{in} = 10\,m\,s^{-1}$) and no reversal flow able to produce a negative moment is observed in the central cavity. The aerodynamic phenomena characterizing the closed cavity increase the air flow impulsion and the rotor's moment without deteriorating the wind turbine's aerodynamical performance. For the static configuration (rotor stopped), the flow in the cavity is also divided into two main directions: near the left wall, due to the deflector orientation, and through the uncovered part of the turbine, at an angle α of about 150°. This is shown in Figure 9 for $U_{in} = 10\,m\,s^{-1}$ and that remains valid for all the treated U_{in} values (Figure 5). The rest of the domain is characterized by a very low intensity flow.

The air mass balance has been carried out systematically in direction "x" for both static and dynamic configurations. This parameter was used to check the convergence of the calculations in addition to the impulsion as previously specified. The convergence criteria is set to 10^{-5}. Distribution of the air mass flow for the dynamic case $Q_{x,\,d}$ is presented in Figure 10 at sections 1 to 6 for $U_{in} = 10\,m\,s^{-1}$.

In the original wind mill version (without cover), a significant part of the air mass flow is evacuated through the top of the assembly between the inlet section

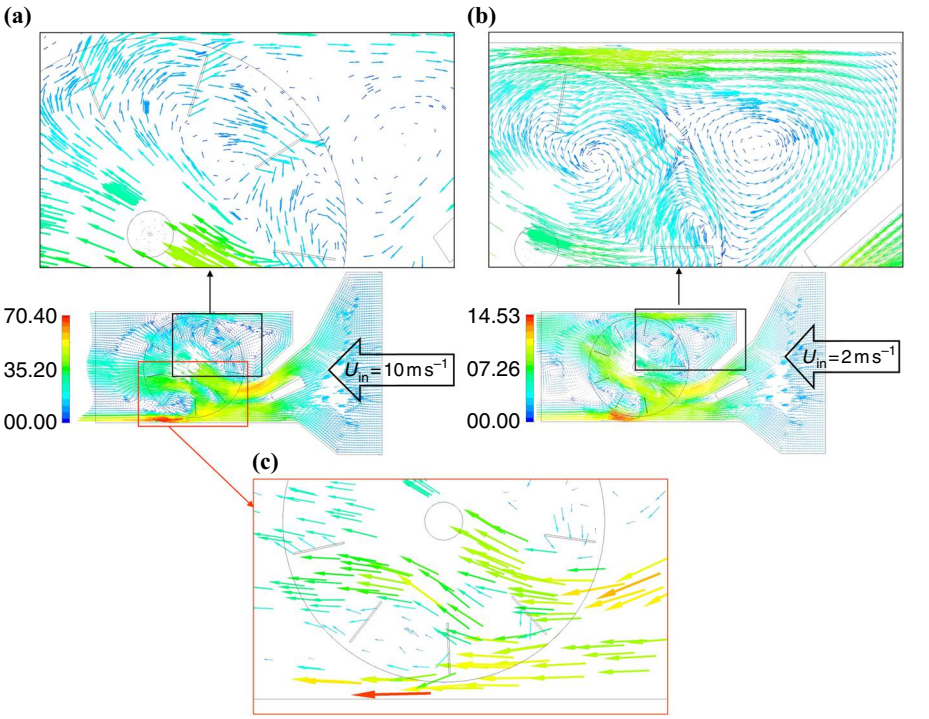

Figure 8.
Details of dynamic wind turbine

Notes: (a) The vortex for U_{in}=10 m s^{-1} (b) the vortex for U_{in}=2 m s^{-1} (c) the flow on the blades 1, 2, 3, 8 and 9 for U_{in}=10 m s^{-1}

(section 7) and section 6, upstream of the deflector. In the dynamic configuration, only 42 percent of the air mass collected in section 7 is effectively admitted into the central cavity, where 61 percent and this part is lost through the top. Finally, a maximum of 17 percent of the air mass collected in section 7 (input) contributes to produce the rotor's torque.

It should nevertheless be noted that the flow characteristics in the closed version could have a negative impact on the wind turbine's operation. Indeed, if the pressure exerted by the flow on the blades increases the rotor's torque, collateral counterproductive effects could occur, as increasing rotor's vibration, friction rotor-bearings, excessive forces on the materials of the blades, etc. These consequences should be examined by a particular study.

4. Conclusion

This study examines the aerodynamical phenomena that occur in one of the original versions of Sistan wind mill, modified by the installation of a cover on the whole assembly top. This work complements the sudy by Baïri *et al.* (2016) considering the

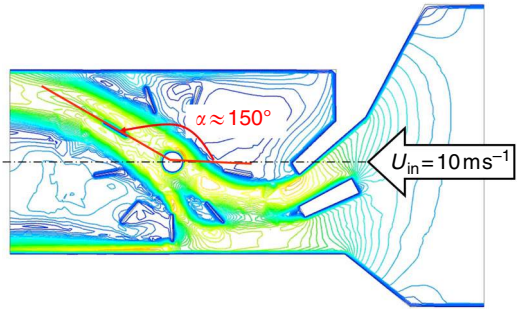

Note: $U_{in} = 10\,\mathrm{m\,s^{-1}}$

Figure 9.
The two main airflow directions for the static wind turbine

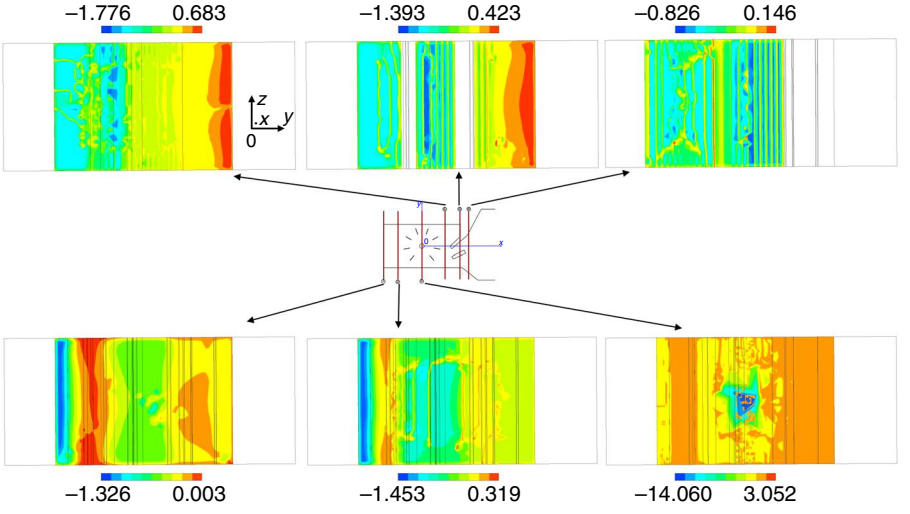

Figure 10.
Distribution of the air mass flow $Q_{x,\,d}$ at sections 1-6 for the dynamic wind turbine and $U_{in} = 10\,\mathrm{m\,s^{-1}}$

same assembly without the cover. The modification which can be easily realized, is proposed to improve the performance of the original wind mill version. Calculations are done for inlet velocities varying from 2 to 10 m s^{-1}, by means of the finite volume method associated to the realizable k-ε turbulence model. The computational domain consists of a rotating sub domain including the wind turbine equipped with nine blades and a fixed sub domain including the rest of the computational domain. Both are connected by means of a sliding mesh interface. The modified version provides a significant increase in the air flow's impulsion within the central active cavity. The maximum velocity can reach 70.40 m s^{-1} for an inlet velocity of 10 m s^{-1} in the dynamic configuration (operating wind mill), while only 20.53 m s^{-1} are observed for this maximum value in the original version in the same conditions. The cover avoids the significant loss of air mass through the top of the assembly, on average of about 83 percent of the quantity collected at the assembly inlet. Examination of the local aerodynamic phenomena shows that when vortices are present in the central cavity, they do not disturb the wind turbine operation given their position and very low intensity. In all cases, they rotate in the same direction as the rotor. Their possible presence does not degrade the aerodynamic performance of the wind turbine that are greatly improved in the proposed version. It is nevertheless important to note that the significant increase in air mass impulsion may be accompanied by adverse effects on the integrity, functioning and sustainability of the wind mill. The vibrations that may be induced, the increased axis-bearings friction and the strength of the materials used in the assembly must be studied. It is also necessary to consider the heat transfer occurring throughout the assembly and the associated changes in air properties, as this study is made in isothermal conditions. The temperature variations can be important in regions where these wind mills may be installed, and the wind mill's aerodynamic performance may be significantly dependent on temperature conditions.

References

Abadie, M.O. and Mendes, N. (2008), "Numerical assessment of turbulence effect on the evaluation of wind-driven rain specific catch ratio", *International Communications in Heat and Mass Transfer*, Vol. 35, pp. 1253-1261.

Al-Hassan, A.Y. and Hill, D.R. (1986), *Islamic Technology: An Illustrated History*, Cambridge Press, Cambridge University, Cambridge.

Almohammadi, K.M., Ingham, D.B., Ma, L. and Pourkashan, M. (2013), "Computational fluid dynamics (CFD) mesh independency techniques for a straight blade vertical axis wind turbine", *Energy*, Vol. 58, pp. 483-493.

Altan, B.D. and Atılgan, M. (2008), "An experimental and numerical study on the improvement of the performance of Savonius wind rotor", *Energy Conversion and Management*, Vol. 49, pp. 3425-3432.

Anderson, J.D. (1995), *Computational Fluid Dynamics: The Basics with Applications*, 6th ed., ISBN: 0070016852, McGraw Hill.

ANSYS, CFX v14 Help Manuals (2011), "Solver theory", available at: http://dx.doi.org/www.ansys.com/cfx

Arfaie, A., Burns, A.D., Dorrell, R.M., Eggenhuisen, J.T., Ingham, D.B. and McCaffrey, W.D. (2014), "Optimised mixing and flow resistance during shear flow over a rib roughened boundary", *International Communications in Heat and Mass Transfer*, Vol. 58, pp. 54-62.

Baïri, A. (2014), "Aerodynamic phenomena in the channel of a large VAWT", *Symposium on Renewable Energy Applications and Development, Proceedings of SREAD, Paris, March 12-15*, pp. 47-55.

Baïri, A., San Martín, D., Laraqi, N., Alilat, N., Bauzin, J.G. and Hocine, A. (2015), "Review of the main turbulence models used in thermal and aerodynamical problems", *Invited Conference in International Symposium on Numerical Methods in Thermal Engineering and Aerodynamics, Proceedings of ISNMTEA, San Sebastian (Spain), August 10-13*, pp. 38-52.

Baïri, A., San Martín, D., Baïri, I., Adeyeye, K., She, K., Hocine, A., Alilat, N., Bauzin, J.G., Lamriben, C., Chanetz, B. and Laraqi, N. (2016), "Aerodynamics in the open channel of the Sistan-type wind-mill with vertical axis wind turbine", *International Journal of Numerical Methods for Heat & Fluid Flow* (in press).

Bhutta, M.M.A., Hayat, N., Farooq, A.U., Ali, Z., Jamil, S.R. and Hussain, Z. (2012), "Vertical axis wind turbine. A review of various configurations and design techniques", *Renewable and Sustainable Energy Reviews*, Vol. 16, pp. 1926-1939.

Cao, L., Wang, H., Jia, Y., Wang, Z. and Yuan, W. (2012), "Analysis on the influence of rotational speed to aerodynamic performance of vertical axis wind turbine", *International Conference on Advances in Computational Modeling and Simulation, Procedia Engineering*, Vol. 31, pp. 245-250.

Campbell, J.L. (2011), "Architecture and identity: the occupation, use, and reuse of Mughal Caravanserais", PhD thesis, Department of Anthropology, University of Toronto, Toronto.

Cohen, Y. and Ryan, P.A. (1985), "Mass transfer across wind-sheared interfaces", *International Communications in Heat and Mass Transfer*, Vol. 12, pp. 139-148.

Hau, E. (2006), *Wind Turbines – Fundamentals, Technologies, Application, Economics*, 2nd ed., Springer-Verlag, Berlin, Heidelberg.

Howell, R., Qin, N., Edwards, J. and Durrani, N. (2010), "Wind tunnel and numerical study of a small vertical axis wind turbine", *Renewable Energy*, Vol. 35, pp. 412-422.

Islam, M., Ting, D.S.K. and Fartaj, A. (2008), "Aerodynamic models for Darrieus-type straight-bladed vertical axis wind turbines", *Renewable and Sustainable Energy Reviews*, Vol. 12, pp. 1087-1109.

Irabu, K. and Roy, J.N. (2007), "Characteristics of wind power on Savonius rotor using a guide-box tunnel", *Experimental Thermal and Fluid Science*, Vol. 32, pp. 580-586.

Joselin Herberta, G.M., Iniyan, S., Sreevalsan, E. and Rajapandian, S. (2007), "A review of wind energy technologies", *Renewable and Sustainable Energy Reviews*, Vol. 11, pp. 1117-1145.

Kadja, M., Anagnostopoulos, J.S. and Bergeles, G.C. (1996), "Study of wind flow and pollutant dispersion by newly developped precision-improving methods", *International Communications in Heat and Mass Transfer*, Vol. 23 No. 8, pp. 1065-1076.

Kim, D. and Gharib, M. (2013), "Efficiency improvement of straight-bladed vertical-axis wind turbines with an upstream deflector", *Journal of Wind Engineering and Industrial Aerodynamics*, Vol. 115, pp. 48-52.

Liou, T.M., Hwang, J.J. and Chen, S.H. (1993), "Simulation and measurement of enhanced turbulent heat transfer in a channel with periodic ribs on one principal wall", *International Journal of Heat and Mass Transfer*, Vol. 36, pp. 507-517.

Lin, S.Y. and Shieh, T.H. (2010), "Study of aerodynamical interference for a wind turbine", *International Communications in Heat and Mass Transfer*, Vol. 37, pp. 1044-1047.

McTavish, S., Feszty, D. and Sankar, T. (2012), "Steady and rotating computational fluid dynamics simulations of a novel vertical axis wind turbine for small-scale power generation", *Renewable Energy*, Vol. 41, pp. 171-179.

Muller, G., Mark, F., Jentsch, M.F. and Stoddart, E. (2009), "Vertical axis resistance type wind turbines for use in buildings", *Renewable Energy*, Vol. 34, pp. 1407-1412.

Okamoto, S., Seo, S., Nakaso, K. and Kawai, I. (1993), "Turbulent shear flow and heat transfer over the repeated two-dimensional square ribs on ground plane", *Journal of Fluids Engineering*, Vol. 115, pp. 631-637.

Rapin, M. and Noël, J.M. (2010), *Énergie éolienne – Principes Études de cas*, ISBN 10:2100508016/ ISBN 139782100508013, Dunod Editeur.

Rapin, M. and Noël, J.M. (2014), *Énergie éolienne. Du petit éolien à l'éolien off shore*, ISBN2100597124, EAN13: 9782100597123, Technique et Ingénierie, Dunod/L'Usine Nouvelle.

Shepherd, D.G. (1990), "Historical development of the windmill", NASA Contractor Report No. 4337, DOE/NASA/5266-1.

Sharpe, T. and Proven, G. (2010), "Crossflex: concept and early development of a true building integrated wind turbine", *Energy and Buildings*, Vol. 42, pp. 2365-2375.

Versteeg, H.K. and Malalasekara, W. (1995), *An Introduction to Computational Fluid Dynamics. The Finite Volume Method*, ISBN 0-582-21884-5, Pearson Education Limited.

Corresponding author
Professor Abderrahmane Baïri can be contacted at: bairi.a@gmail.com